Ingeniare. Revista chilena de ingeniería, (2025) 33:1

Synthesis of fibrous silica BEA for methanol to olefin reaction

Síntesis de sílica fibrosa BEA para reacciones de metanol a olefina

M.H.M. Sofi[1*] https://orcid.org/0000-0003-4431-8996
M.Y.S. Hamid[2] https://orcid.org/0000-0003-4770-1392
A.A. Jalil[2] https://orcid.org/0000-0003-0811-3168

Recibido 14 de octubre de 2024, aceptado 17 de marzo de 2025
Received: October 14, 2024 Accepted: March 17, 2025

ABSTRACT

Traditional methods of producing olefins largely depend on petroleum fuels, significantly contributing to environmental and sustainability challenges. The Methanol-to-Olefin (MTO) process is a sustainable alternative for producing olefin products, utilizing abundant materials like CO_2, coal, natural gas, and biomass. However, the catalytic efficiency of the MTO process utilizing conventional zeolite catalysts is restricted by their relatively low activity, primarily attributable to the zeolite's microporous shape and high acidity. This study successfully synthesized Beta zeolite featuring a fibrous silica structure using a combination of microemulsion and zeolite seed-assisted methods. The catalysts were characterized using field emission scanning electron microscopy (FESEM), Fourier transform infrared spectroscopy-potassium bromide (FTIR-KBr), nitrogen physisorption, and ammonia-temperature programmed desorption (NH_3-TPD). The fibrous silica Beta (HFBEA) appears to have a highly organized spherical structure and a consistent distribution of particle sizes, as confirmed by FESEM analysis. FTIR-KBr further confirms the formation of fibrous silica of synthesized HFBEA while maintaining the framework of Beta seed. Surface analysis revealed that HFBEA has a 35% higher BET-specific surface area and an 86% greater volume of mesopore in comparison to conventional HBEA. NH_3-TPD results indicate that incorporating fibrous silica into the BEA structure significantly reduced the catalyst's acidity. These factors contributed to the outstanding catalytic performance of HFBEA in the MTO process, achieving 95.4% methanol conversion and demonstrating significant selectivity towards light olefins at 78.1%, outperforming the commercial HBEA catalyst.

Keywords: Methanol to olefin, unique morphology, beta zeolite, fibrous silica material, mesoporous.

RESUMEN

Los métodos tradicionales de producción de olefinas dependen en gran medida de los combustibles derivados del petróleo, que suponen un reto importante para el medio ambiente y la sostenibilidad. El proceso de metanol a olefina (MTO) es una alternativa sostenible para la producción de olefinas, utilizando materiales abundantes comoCO_2*, carbón, gas natural y biomasa. Sin embargo, la eficiencia catalítica del proceso MTO utilizando catalizadores de zeolita convencionales está restringida por su*

[1] Universiti Teknologi Malaysia. Faculty of Chemical and Energy Engineering. Johor Bahru, Johor, Malaysia.
Email: hafizuddin-1998@graduate.utm.my
[2] Institute of Future Energy. Centre of Hydrogen Energy. Johor Bahru, Johor, Malaysia.
Email: m.yusuf@utm.my; r-aishahj@utm.my
* Autor de correspondencia: m.yusuf@utm.my

relativamente baja actividad, que se atribuye principalmente a la forma microporosa de la zeolita y a su alta acidez. En el presente estudio, la zeolita Beta con estructura de sílice fibrosa se ha obtenido mediante una combinación de métodos de microemulsión y de semilla de zeolita. Los catalizadores se caracterizaron mediante microscopía electrónica de barrido por emisión de campo (FESEM), espectroscopía infrarroja por transformada de Fourier-bromuro de potasio (FTIR-KBr), fisisorción de nitrógeno y desorción programada de amoníaco a temperatura (NH_3-TPD). La sílica fibrosa Beta (HFBEA) presenta una estructura esférica muy organizada y una distribución uniforme del tamaño de las partículas, como confirma el análisis FESEM. El FTIR-KBr confirma además la formación de sílice fibrosa de la HFBEA sintetizada, manteniendo la estructura de la semilla Beta. El análisis de la superficie reveló que la HFBEA tiene un 35% más de superficie específica BET y un 86% más de volumen de mesoporo en comparación con la HBEA convencional. Los resultados de NH_3-TPD indican que la incorporación a la estructura de BEA de sílica fibrosa reduce significativamente la acidez del catalizador. Estos factores contribuyeron al excelente rendimiento catalítico del HFBEA en el proceso MTO, alcanzando una conversión de metanol del 95,4% y demostrando una selectividad significativa hacia las olefinas ligeras del 78,1%, superando al catalizador HBEA comercial.

Palabras clave: Metanol a olefina, morfología única, zeolita beta, material de sílice fibrosa, mesoporoso.

INTRODUCTION

Ethylene and propylene, essential light olefins in the petrochemical industry, play a crucial role in producing a wide array of products such as polyethylene, acrylic acid, polypropylene, ethylene oxide, ethyl chloride, propylene oxide, and numerous other chemical intermediates [1]. Currently, the generation of light olefins relies heavily on energy-demanding processes predominantly based on fossil fuels. The primary methods include steam cracking of crude oil and catalytic cracking, which are highly reliant on the availability and cost of fossil fuel resources [2], [3]. Additionally, major chemical processing, including ethylene and propylene production from petroleum fuels, generated around 935 million metric tons of direct CO_2 emission in 2022 [4]. This traditional manufacture of light olefins, dependent on petroleum, can provide substantial environmental challenges.

Methanol to olefins (MTO) signifies a substantial paradigm shift, offering a proven non-petrochemical route. Unlike conventional feedstocks sourced directly from fossil resources, methanol serves as a distinct feedstock in this process [5], [6]. This approach has acquired importance among worldwide catalytic processes due to its capacity to serve the growing need for light olefins [7]. Since its initial discovery, the MTO reaction has utilized a range of zeolite materials, primarily acidic zeolites, since the product spectrum of the MTO reaction is highly influenced by the pore size, crystal size, and acidity of the catalyst material used [8]-[10]. In addition, zeolites exhibit outstanding selectivity in producing light olefins, owing to their excellent shape selectivity and the unique properties of their active sites [11]-[13].For instance, due to its moderate acidity and tiny pore aperture SAPO-34 can generate substantial amounts of light olefins, such as ethylene and propylene. However, its catalytic performance is limited by a short catalytic lifetime due to fast carbon formation [5], [14].

In contrast, ZSM-5, with high acidity and moderate pore sizes, offers enhanced resistance to catalyst deactivation compared to SAPO-34. However, its firm acidity slightly reduces its selectivity for ethylene and propylene [15]. Given the limitations of SAPO-34 and ZSM-5, it is imperative to explore new potential zeolites to remarkable catalysts that exhibit excellent light olefins selectivity and prolonged catalytic lifetimes for converting methanol to olefins.

Beta zeolites demonstrate great potential as catalysts for MTO reactions compared to other natural and synthetic zeolites; this is because the other recently developed zeolites, except SAPO-34 and ZSM-5, have not yet been commercially adopted due to uncertainties about their scalability in synthesis and applicability in established industrial processes [16]. However, the microporous structure of conventional Beta catalysts restricts their catalytic activity by limiting active site accessibility and thereby reducing overall catalytic activity. One effective approach involves reducing the diffusion path for reactants and products within zeolites by integrating mesopores into their framework to overcome this limitation [17], [18].

In this study, fibrous silica Beta was prepared to combine the microporous Beta zeolite with the external mesoporous structure of fibrous silica. This approach aims to increase the number of active sites and enhance the mass transport of methanol, light olefins, and additional hydrocarbon compounds into and out of the zeolite pores; no studies exploring the use of fibrous silica Beta materials in the MTO process to date. However, prior research demonstrated that the formation of a dense dendritic fibrous silica layer around zeolite Beta increases interparticle porosity and results in a large BET surface area; this, in turn, provides more sites for the adsorption of reactant molecules, hence enhancing the catalytic reaction of CO methanation [19]. The use of fiber silica Beta material has been found to have comparable outcomes in diverse catalytic reactions, including CO_2 methanation [20], benzene methylation reaction with toluene [21], and cyclic and noncyclic alkane isomerization [22].

MATERIALS AND METHODS

Materials

The conventional Beta zeolite was purchased from Zeolyst International, Inc, while toluene (98%), butanol (98%), methanol (99.5%), urea (99.5%), cetyltrimethylammonium bromide (>98%, CTAB), tetraethyl orthosilicate (>98%, TEOS), and ammonium nitrate (NH_4NO_3) were acquired from Merck. The nitrogen gas tanks, consisting of 99.5% N_2, and the compressed air tanks, with over 90% air composition, were acquired from Mega Mount Industrial Gases. All chemicals utilized were of analytical quality and employed without any purifying procedures.

Catalyst synthesis

The fibrous silica Beta was prepared via microemulsion combined with a Beta zeolite-seed assisted technique, following procedures outlined in the literature [23], [24]. The catalyst was synthesized with specific weight ratios of urea/Beta = 2.36, CTAB/Beta = 3.95, toluene/Beta = 102, butanol/Beta = 4.77, H_2O/Beta = 110, and TEOS/Beta = 8.37. First, a water, CTAB, and urea solution was stirred using a magnetic stirrer at room temperature for 30 minutes in a Teflon vessel. Next, a precise quantity of toluene and butanol was introduced into the solution. Once a homogeneous mixture was achieved, Beta zeolite seed was introduced, and TEOS was added dropwise, followed by vigorous stirring for 4 hours. The resulting mixture was then heated in an oven at 120 ºC and 1 atm pressure for 6 hours to facilitate the aging process. Following this, the solution was moved from the Teflon vessel to a beaker and dried in an oven at 110 ºC for one night. Afterward, the dried sample was subjected to calcination in a furnace at a temperature of 550 ºC for 6 hours. The resulting sample was designated as FBEA.

The FBEA and BEA catalyst was turned into the H-form (protonated) by a dual consecutive ion exchange, which was performed utilizing 2 g of the parent sample. The sample underwent treatment with 10.51 g of NH_4NO_3 salt dissolved in 100 ml of deionized water. The mixture was then agitated at 50 ºC for 8 hours. The resulting mixture underwent filtration via a filter paper and funnel, then washed repeatedly with deionized water and subsequently subjected to drying in an oven at 110 ºC overnight. Afterward, it undergoes calcination in air at a temperature of 550 ºC for 3 hours. The H-form fibrous silica Beta and conventional Beta samples will be referred to as HFBEA and HBEA, respectively.

Catalytic activity

The conversion of methanol to olefins was carried out in a micro-catalytic pulse reactor operating at a pressure of 1 atm. The reactor was fitted with an online collecting valve for gas chromatographic examination. Here, 0.25 g of the prepared sample was packed into an 8 mm stainless steel tube using glass wool to hold the catalyst. Prior to the reaction, the sample underwent a pre-treatment process to activate the catalyst and eliminate impurities; this involved exposing the catalyst to air at a flow rate of 60 ml/min and heating it to a temperature of 450 ºC for 1 hour. Methanol was injected into the reactor at a 60 ml/min nitrogen flow rate at various temperatures ranging from 300 to 500 ºC. The reactor effluent was directed through gas chromatography (Agilent GC 7820A-FID), which was attached to an HP-5 capillary column to analyze the product composition after the catalytic reaction. The following equations, equation (1) and equation (2), were applied to calculate the conversion of the reactant ($X_{methanol}$) and the selectivity of the desired product (S_{LO}):

$$X_{methanol} = \frac{n_{Min} - n_{Mout}}{n_{Min}} \times 100\% \tag{1}$$

$$S_{LO} = \frac{n_{Clo}}{\sum n_{Ch}} \times 100\% \tag{2}$$

Where n_{Min}, n_{Mout}, n_{Clo}, and n_{Ch} indicate moles of reactant feed, unreacted reactant, total ethylene and propylene gases, and undesired hydrocarbon gases, respectively.

RESULTS AND DISCUSSIONS

Morphological studies

Figure 1 depicts the microscopic morphology of HBEA and HFBEA samples as analyzed by field emission scanning electron microscopy (FESEM). As can be seen, the surface morphology and overall structure of HBEA have changed from irregular clustered shapes (Figure 1a) to well-defined spherical micro-nanospheres resembling cockscomb structures. These structures exhibit uniform particle sizes ranging from 300 to 400 nm, suggesting the presence of bi-continuous lamellar silica fibers (Figure 1b). The surface shape and texture of HFBEA closely resembled those of KAUST Catalysis Center-1 (KCC-1), which was first introduced by Polshettiwar, Cha, Zhang, and Basset, and similar to other fibrous silica Beta observed in a prior study [20], [24], [25]. The formation of the cockscomb-shaped morphology is likely due to the synergistic interactions among surfactant (CTAB), hydrolyzing agent (urea), oil phase solvent (toluene), hydrophilic solvent (water), and co-surfactant (butanol) during the microemulsion process. These interactions were essential in promoting the formation of the compact dendritic silica fiber zeolite material [20].

Vibrational spectroscopy

The Fourier transform infrared spectroscopy-potassium bromide (FTIR-KBr) method was employed to analyze the chemical properties of both HBEA and HFBEA. Figure 2 illustrates the FTIR spectrum in the 1400 - 400 cm^{-1} wavenumber range. Both catalysts show a similar sequence of vibrational peaks, detected at 1230, 1084, 970, 800, 620, 545, and 463 cm^{-1}. The initial segment comprises four distinct peaks detected at 1230, 1084, 800, and 463 cm^{-1}, corresponding to the external and internal asymmetric stretching, symmetric stretching, and bending vibrations of T-O-T (where T represents Si and Al) within the framework, respectively [23].The peak at 970 cm^{-1} is attributed to the external silanol group (Si-OH) [26], [27].The peaks observed at 620 and 545 cm^{-1}, respectively, confirmed the existence of five- and six-membered rings within the Beta catalyst framework [24]. The synthesized HFBEA shows a higher intensity, which is dominated by a strong band at 1084 cm^{-1}, 800 cm^{-1}, and 463 cm^{-1}, and an additional peak at 970 cm^{-1}. This confirms the presence of silica fibers surrounding the Beta seed, as evident in FESEM results (Figure 1). These results confirmed the successful synthesis of HFBEA while maintaining the framework of Beta seed.

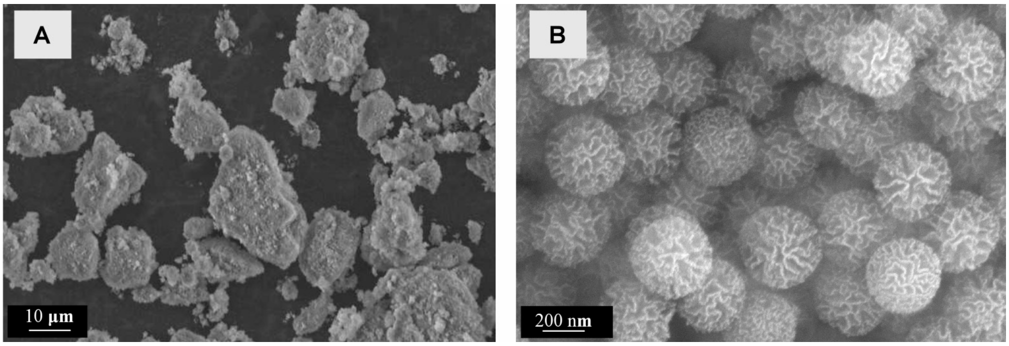

Figure 1. FESEM image of a) HBEA and b) HFBEA.

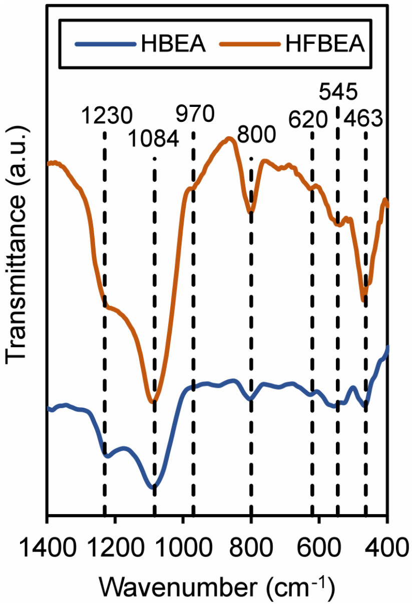

Figure 2. FTIR-KBr spectra of HBEA and HFBEA.

Surface analysis

The catalyst's textural properties were thoroughly analyzed using the N_2 adsorption-desorption technique. Figure 3a depicts the N_2 physisorption isotherms of HBEA and HFBEA. According to the isotherms graph, HFBEA has a greater nitrogen uptake than HBEA at higher relative pressure (P/Po between 0.8 to 1.0), implying the existence of a higher number of mesopores. These outcomes are further evident when the non-local density functional theory (NLDFT) approach is applied, which was employed to obtain the pore size distributions of HBEA and HFBEA. A peak within the less than 2 nmrange signifies the existence of micropores, whereas a peak within the greater than 2 nm range indicates the presence of mesopores. Both samples exhibit a micro-mesoporous structure, as demonstrated in Figure 3b. However, in HFBEA, there is a reduced peak within the micropore range and an elevated peak within the mesopore range.

Overall, HBEA exhibited a BET-specific surface area of 405 m²/g and a total pore volume of 0.8 cm³/g, while HFBEA showed a BET-specific surface area of 547 m²/g and a total pore volume of 1.4 cm³/g. In HFBEA, mesopores dominate with a 1.3 cm³/g volume, comprising 93% of the total pore volume. Conversely, HBEA exhibits a mesopore volume of approximately 7 cm³/g, constituting 87.5% of the total pore volume. The increased surface area and volume of mesopores in HFBEA can be attributed to a bi-continuous lamellar silica framework produced within the catalyst. The textural characteristics of both catalysts were examined, concluding that the microemulsion, coupled with the seed-assisted synthesis method, is effective in creating mesoporosity while maintaining microporosity.

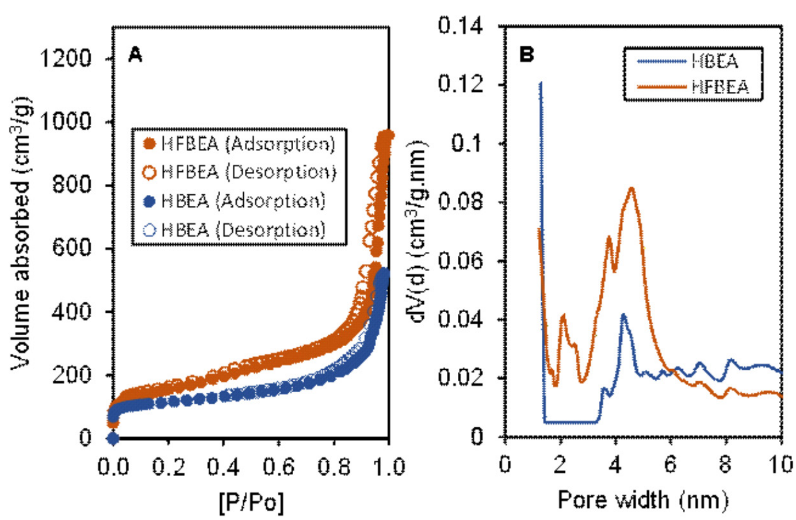

Figure 3. a) N2 physisorption isotherm and b) pore size distribution of HBEA and HFBEA.

Acidic properties

The ammonia-temperature programmed desorption (NH_3-TPD) technique was utilized to examine the acidities of the catalysts throughout a temperature range of 100 to 500 ºC. The NH_3-TPD peaks of prepared catalysts were analyzed using Gaussian curve fitting, with the dashed curve representing the summation of fitted Gaussian curves. Figure 4 illustrates that the NH_3-TPD curves before and after the deconvolution for all the samples exhibit comparable patterns and can be divided into two primary regions. The first region is a desorption peak occurring at low temperatures, specifically between 100 and 300 ºC. This band is associated with ammonia weakly bonded on defect sites such as n-OH (where n represents Si, Al, and P). The second part is a band observed at higher temperatures, ranging from 300 to 500 ºC. This band corresponds to ammonia adsorbed on strong bridge hydroxyl Si-(OH)-Al acidic groups [28]-[30]. The desorption peak areas of the weak and strong acid sites for HFBEA are lower than those of HBEA, indicating a reduction in both types of acid sites.

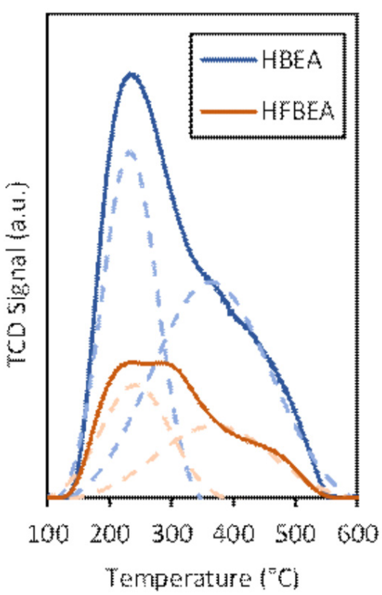

Figure 4. NH3-TPD profiles for HBEA and HFBEA catalysts. The bold curves represent the raw experimental data, while the dashed line corresponds to the individual component curves of acid sites obtained through Gaussian peak deconvolution.

This observation of the acidities indicates that the formation of fibrous silica on the BEA catalyst significantly reduced the acidity of the samples since the fibrous silica framework is composed solely of silica, which lacks surface acidity [31]. Furthermore, the acidity of aluminosilicate zeolite is closely related to its silica-to-alumina (Si/Al) ratio; changes in this ratio can significantly influence its overall acidity [32], [33]. Thus, introducing fibrous silica into the zeolite BEA framework resulted in a high Si/Al ratio, which decreased the abundance of acid sites and subsequently reduced the overall acidity of the catalyst.

Catalytic activity

The comparative catalytic activities of HFBEA and commercial HBEA catalysts are illustrated in Figure 5, showing methanol conversion, total light olefin selectivity(Figure 5a), and product distribution (ethylene and propylene) across various reaction temperatures. It was noted that both HFBEA and HBEA catalysts exhibited higher methanol conversion and hydrocarbon selectivity with increasing reaction temperature.

Despite the HFBEA sample operating at a lower reaction temperature of 300 ºC, it displays enhanced catalytic activity, reaching a methanol conversion rate of 80.7% and a total light olefin selectivity of 22%. By contrast, the conventional HBEA catalyst exhibited a conversion rate of 75.1% and a selectivity of 10% under the same conditions. Similarly, when exposed to elevated reaction temperatures of 500 ºC, HFBEA demonstrates notable catalytic efficiency, achieving a methanol conversion rate of 95.4% and a selectivity of 78.1% towards light olefins; this represents an improvement of 3.3% and 4% compared to the HBEA catalyst. Regarding ethylene and propylene distribution, HFBEA displays a similar trend to HBEA, with ethylene emerging as the predominant product as the reaction temperature increases and reaches the highest production at 500 ºC, as depicted in Figure 5b and Figure 5c. Nevertheless, HFBEA exhibits superior selectivity towards ethylene and propylene across all reaction temperatures compared to HBEA.

The enhanced catalytic activity can be attributed to modifying the physicochemical characteristics of HFBEA. The introduction of a mesoporous structure in HFBEA, as illustrated in the N_2

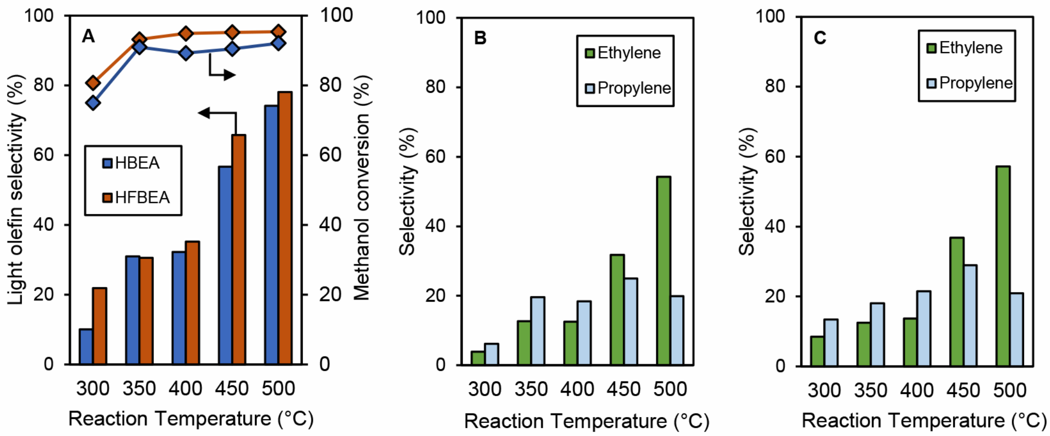

Figure 5. a) Methanol conversion and total light olefin selectivity for HBEA and HFBEA, and product distribution of b) HBEA and c) HFBEA catalysts.

adsorption-desorption data (Figure 3), effectively mitigates the diffusion constraints inherent in the commercial Beta material's micropores. The superior diffusion properties of HFBEA are advantageous in MTO reactions. They facilitate efficient mass transport of methanol molecules and diffusion of more significant hydrocarbon compounds through the pores, thereby enhancing catalytic performance [34], [35]. Furthermore, the decrease in the number of acid sites in this sample, as indicated in the NH_3-TPD analysis (Figure 4), is crucial for enhancing light olefin formation; this is because decreasing the number of acid sites in catalysts has advantages in terms of minimizing undesirable reactions, such as olefin aromatization, in MTO processes, thereby reducing the formation of bulkier hydrocarbon by-products [36]. These factors contribute to the excellent catalytic performance of HFBEA.

CONCLUSIONS

In conclusion, fibrous silica Beta (HFBEA) was effectively synthesized using a combination of microemulsion and seed-assisted methods. The physicochemical attributes of the prepared sample were evaluated using different characterization techniques, such as FESEM, N_2 adsorption-desorption, and NH_3-TPD. The characterization outcomes indicated that HFBEA exhibited uniform spherical morphology, offering increased surface area and mesopore volume while reducing acidity. Based on its catalytic performance, the HFBEA catalyst shows a significant improvement in methanol conversion, achieving 95.4%, and exhibits a high selectivity for light olefins at 78.1%, surpassing the commercial HBEA catalyst, which achieves 92.1% conversion and 74.1% selectivity. The formation of mesoporous structure and the reduction in the amount of acid sites in HFBEA are responsible for these outcomes. These discoveries signify a notable progression in advancing effective catalysts for producing light olefins, offering potential benefits for the petrochemical sector and the environment.

ACKNOWLEDGEMENTS

As authors, we gratefully acknowledge the financial support provided by the Ministry of Higher Education under the Fundamental Research Grant Scheme, UTM, FRGS/1/2022/STG05/UTM/02/11.

REFERENCES

[1] C.S. Hsu and P.R. Robinson, "*Petroleum Science and Technology*," *Petrochemicals*, Springer: Cham, Switzerland, 2019, pp. 345-383, doi: 10.1007/978-3-030-16275-7_16.

[2] Z. Gholami, F. Gholami, Z. Tišler, and M. Vakili, "A review on the production of light olefins using steam cracking of hydrocarbons," *Energies*, vol. 14, 2021, doi: 10.3390/en14238190.

[3] Y. Yoshimura *et al.*, "Catalytic cracking of naphtha to light olefins," *Catalysis Surveys from Japan*, vol. 4, 2001, doi: 10.1023/A:1011463606189.

[4] IEA, "Chemicalsm", iea.org, 2022. Accessed: Oct. 8, 2023. [Online]. Available: https://www.iea.org/energy-system/industry/chemicals

[5] D. Zapater, J. Lasobras, J. Soler, J. Herguido, and M. Menéndez, "MTO with SAPO-34 in a Fixed Bed Reactor: Deactivation Profiles," *Industrial & Engineering Chemistry Research*, vol. 60, no. 45, pp. 16162-16170, 2021, doi:10.1021/acs.iecr.1c02718.

[6] M.R. Gogate, "Methanol-to-olefins process technology: current status and future prospects," *Petroleum Science and Technology*, vol. 37, no. 5, pp. 559-565, 2019, doi:10.1080/10916466.2018.1555589.

[7] I.B. Minova *et al.*, "Silicon redistribution, acid site loss and the formation of a core-shell texture upon steaming SAPO-34 and their impact on catalytic performance in the Methanol-to-Olefins (MTO) reaction," *Journal of Catalysis*, vol. 395, pp. 425-444, 2021, doi:10.1016/j.jcat.2021.01.012.

[8] S. Wang *et al.*, "Methanol to olefins over H-MCM-22 zeolite: Theoretical study on the catalytic roles of various pores," *ACS Catalysis*, vol. 5, no. 2, pp. 1131-1144, 2015, doi:10.1021/cs501232r.

[9] U. Olsbye *et al.*, "Conversion of methanol to hydrocarbons: How zeolite cavity and pore size controls product selectivity," *Angewandte Chemie International Edition*, vol. 51, no. 24, pp. 5810-5831, 2012, doi:10.1002/anie.201103657.

[10] T.R. Koyama *et al.*, "Key role of the pore volume of zeolite for selective production of propylene from olefins," *Physical Chemistry Chemical Physics*, vol. 12, no. 11, pp. 2541-2554, 2010, doi: 10.1039/b921927g.

[11] J. Zhong, J. Han, Y. Wei, and Z. Liu, "Catalysts and shape selective catalysis in the methanol-to olefin (MTO) reaction," *Journal of Catalysis*, vol. 396, pp. 23-31, 2021, doi:10.1016/j.jcat.2021.01.027.

[12] C. Selzer, T. Biemelt, A. Werner, and S. Kaskel, "Hierarchical zeolite ZSM-58 as shape selective catalyst for methanol-to-olefins reaction," *Microporous and Mesoporous Materials*, vol. 261, pp. 51-57, 2018, doi:10.1016/j.micromeso.2017.11.005.

[13] E.C. Umejuru *et al.*, "Application of zeolite based nanocomposites for wastewater remediation: Evaluating newer and environmentally benign approaches," *Environmental Research*, vol. 231, Art. no. 116073, 2023, doi:10.1016/j.envres.2023.116073.

[14] D. Chen, K. Moljord, and A. Holmen, "A methanol to olefins review: Diffusion, coke formation and deactivation on SAPO type catalysts," *Microporous and Mesoporous Materials*, vol. 164, pp. 239-250, 2012, doi:10.1016/j.micromeso.2012.06.046.

[15] X. Jiang *et al.*, "Conversion of methanol to light olefins over nanosized [Fe,Al]ZSM-5 zeolites: Influence of Fe incorporated into the framework on the acidity and catalytic performance," *Microporous and Mesoporous Materials*, vol. 263, pp. 243-250, 2018, doi:10.1016/j.micromeso.2017.12.029.

[16] L. Lin *et al.*, "Control of zeolite microenvironment for propene synthesis from methanol," *Nature Communications*, vol. 12, Art. no. 822, 2021, doi:10.1038/s41467-021-21062-1.

[17] P. Losch *et al.*, "H-ZSM-5 zeolite model crystals: Structure-diffusion-activity relationship in methanol-to-olefins catalysis," *Journal of Catalysis*, vol. 345, pp. 11-23, 2017, doi:10.1016/j.jcat.2016.11.005.

[18] W. Khan, X. Jia, Z. Wu, J. Choi, and A. C.K. Yip, "Incorporating Hierarchy into Conventional Zeolites for Catalytic Biomass Conversions: A Review," *Catalysts*, vol. 9, no. 2, Art. no. 127, 2019, doi:10.3390/CATAL9020127.

[19] I. Hussain, A.A. Jalil, N.A.A. Fatah, S.M. Izan, and M.S. Azami, "Cockscomb-like fibrous silica beta zeolite (FSBEA) as a new engineered catalyst for enhanced CO methanation," *IOP Conference Series: Materials Science and Engineering*, vol. 736, no. 4, Art. no. 042012, 2020, doi:10.1088/1757-899X/736/4/042012.

[20] I. Hussain, A.A. Jalil, S.M. Izan, M.S. Azami, K. Kidam, and N. Ainirazali, "Thermodynamic and experimental explorations of CO2 methanation over highly active metal-free fibrous silica-beta zeolite (FS@SiO2-BEA) of innovative morphology," *Chemical Engineering Science*, vol. 229, Art. no. 116015, 2021, doi:10.1016/J.CES.2020.116015.

[21] A.F.A. Rahman, A.A. Jalil, C.N.C. Hitam, N.S. Hassanm, M. Mohamed, and H.U.

Hambali, "Influence of dendrimeric silica BEA zeolite towards acidity and mesoporosity for enhanced benzene methylation," *Materials Today Proceedings*, vol. 42, pp. 211-216, 2021, doi:10.1016/J.MATPR.2020.11.589.

[22] S.M. Izan, A.A. Jalil, C.K.N.L.C.K. Hitam, and W. Nabgan, "Influence of Nitrate and Phosphate on Silica Fibrous Beta Zeolite Framework for Enhanced Cyclic and Noncyclic Alkane Isomerization," *Inorganic Chemistry*, vol. 59, no. 3, pp. 1723-1735, 2020, doi:10.1021/acs.inorgchem.9b02914.

[23] S.M. Izan *et al.*, "Additional Lewis acid sites of protonated fibrous silica@BEA zeolite (HSi@BEA) improving the generation of protonic acid sites in the isomerization of C_6 alkane and cycloalkanes," *Applied Catalysis A: General*, vol. *570*, pp. 228-237, 2019, doi: 10.1016/j.apcata.2018.11.028.

[24] N.N.M. Ghani *et al.*, "Tailored mesoporosity and acidity of shape-selective fibrous silica beta zeolite for enhanced toluene co-reaction with methanol," *Chemical Engineering Science*, vol. 193, pp. 217-229, 2019, doi:10.1016/J.CES.2018.09.009.

[25] V. Polshettiwar, D. Cha, X. Zhang, and J.M. Basset, "High-surface-area silica nanospheres (KCC 1) with a fibrous morphology," *Angewandte Chemie International Edition*, vol. 49, no. 50, pp. 9652-9656, 2010, doi:10.1002/anie.201003451.

[26] M.S. Azami, A.A. Jalil, N.S. Hassan, I. Hussain, A.A. Fauzi, and M.A.A. Aziz, "Green carbonaceous material-fibrous silica-titania composite photocatalysts for enhanced degradation of toxic 2 chlorophenol," *Journal of Hazardous Materials*, vol. 414, Art. no. 125524, 2021, doi:10.1016/j.jhazmat.2021.125524.

[27] M.B. Bahari *et al.*, "Enriching the methanol generation via CO2 photoconversion over the cockscomb-like fibrous silica copper," *Fuel*, vol. 328, Art. no. 125257, 2022, doi:10.1016/j.fuel.2022.125257.

[28] S. Soltanali and J.T. Darian, "Synthesis of mesoporous SAPO-34 catalysts in the presence of MWCNT, CNF, and GO as hard templates in MTO process," *Powder Technology*, vol. 355, pp. 127-134, 2019, doi:10.1016/j.powtec.2019.07.008.

[29] A.Z. Varzaneh, J. Towfighi, and A. Mohamadalizadeh, "Comparative study of naphtha cracking over SAPO-34 and HZSM-5: Effects of cerium and zirconium on the catalytic performance," *Journal of Analytical and Applied Pyrolysis*, vol. 107, pp. 165-173, 2014, doi:10.1016/j.jaap.2014.02.017.

[30] A. Izadbakhsh, F. Farhadi, F. Khorasheh, and Z.F. Yan, "Effect of heating profile on desorption curve in temperature programmed desorption analysis: Case study of acid sites distribution of SAPO-34," *Journal of Porous Materials*, vol. 16, pp. 599-603, 2009, doi: 10.1007/s10934-008-9237-4.

[31] A. Palčić and V. Valtchev, "Analysis and control of acid sites in zeolites," *Applied Catalysis A: General*, vol. 606, Art. no. 117795, 2020, doi:10.1016/j.apcata.2020.117795ï.

[32] R. Wei, C. Li, C. Yang, and H. Shan, "Effects of ammonium exchange and Si/Al ratio on the conversion of methanol to propylene over a novel and large partical size ZSM-5," *Journal of Natural Gas Chemistry*, vol. 20, no. 3, pp. 261-265, 2011, doi:10.1016/S1003-9953(10)60198-3.

[33] H.W. Huang, Z. Hui, S. H. Zhang, Z. Qiang, and C.Y. Li, "Effect of silicon to aluminum ratio on the selectivity to propene in methanol conversion over H-ZSM-5 zeolites," *Journal of Fuel Chemistry and Technology*, vol. 47, no. 1, pp. 74-82, 2019, doi: 10.1016/S1872-5813(19)30005-2.

[34] Q. Sun, N. Wang, D. Xi, M. Yang, and J. Yu, "Organosilane surfactant-directed synthesis of hierarchical porous SAPO-34 catalysts with excellent MTO performance," *Chemical Communications*, vol. 50, no. 49, pp. 6502-6505, 2014, doi:10.1039/c4cc02050b.

[35] Q. Sun, Z. Xie, and J. Yu, "The state-of-the-art synthetic strategies for SAPO-34 zeolite catalysts in methanol-to-olefin conversion," *National Science Review*, vol. 5, no. 4, pp. 542–558, 2018, doi:10.1093/nsr/nwx103.

[36] X. Zhao *et al.*, "Investigation of methanol conversion over high-Si beta zeolites and the reaction mechanism of their high propene selectivity," *Catalysis Science & Technology*, vol. 7, no. 24, pp. 5882-5892, 2017, doi: 10.1039/c7cy01804e.